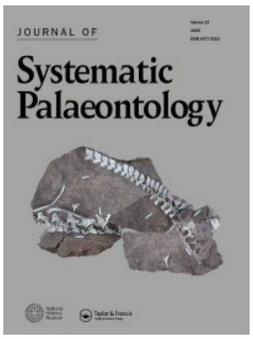

Journal of Systematic Palaeontology

ISSN: 1477-2019 (Print) 1478-0941 (Online) Journal homepage: www.tandfonline.com/journals/tjsp20

New early ruminants (Mammalia: Artiodactyla) from the Oligocene of Nei Mongol (China), with remarks on their phylogenetic relationship

Bian Wang, Qian Wang & Zhao-Qun Zhang

To cite this article: Bian Wang, Qian Wang & Zhao-Qun Zhang (2025) New early ruminants (Mammalia: Artiodactyla) from the Oligocene of Nei Mongol (China), with remarks on their phylogenetic relationship, Journal of Systematic Palaeontology, 23:1, 2552230, DOI: 10.1080/14772019.2025.2552230

To link to this article: https://doi.org/10.1080/14772019.2025.2552230

Journal of Systematic Palaeontology, 2025
Vol. 23, No. 1, 2552230
http://dx.doi.org/10.1080/14772019.2025.2552230

New early ruminants (Mammalia: Artiodactyla) from the Oligocene of Nei Mongol (China), with remarks on their phylogenetic relationship

Bian Wang[a], Qian Wang[a,b,c] and Zhao-Qun Zhang[a,b]*

[a]*Key Laboratory of Vertebrate Evolution and Human Origins, Institute of Vertebrate Paleontology and Paleoanthropology, Chinese Academy of Sciences, Beijing 100044, PR China;* [b]*College of Earth and Planetary Sciences, University of Chinese Academy of Sciences, Beijing 100049, PR China;* [c]*Chongqing Key Laboratory of Resource and Environmental Effects of Major Geological Events, Chongqing Institute of Geology and Mineral Resources, Chongqing 401120, PR China*

(Received 6 June 2024; accepted 24 July 2025)

Ruminants were widely distributed throughout Eurasia and North America from the Eocene to the Oligocene. However, their systematics and early evolution remain obscure. Here, we describe new ruminant specimens collected from late Early Oligocene strata in Nei Mongol, China, identified as *Paragelocus* cf. *scotti* and new species of *Praetragulus* and *Gobiomeryx*. The two new species are the last representatives of their respective genera. We ran a cladistic analysis based on 52 dental and postcranial characters of 30 species. *Praetragulus* is found to be closely related to the North American ruminants *Leptomeryx* and *Hypertragulus*. *Paragelocus*, characterized by a distinct longitudinal lingual cristid on p4, is recovered as a sister taxon to *Pseudomeryx*, forming a monophyletic group with *Gobiomeryx* and *Pseudogelocus*. Including the additional *Lophiomeryx* fossils recently reported, the Saint Jacques–Qianlishan area has now yielded four genera (seven species) of stem ruminants representing three lineages, suggesting a flourishing and complex evolutionary history of early ruminants in Asia during the Oligocene.

https://zoobank.org/urn:lsid:zoobank.org:pub:6409D5F3-BA93-4BE6-8100-70C575C9FC14

Keywords: Eocene–Oligocene transition; Gelocidae; Mongolian Plateau; Ruminantia; Saint Jacques; systematics

Introduction

Ruminantia is the most diverse group of large terrestrial mammals alive today. Extant ruminants are predominantly pecorans, while non-pecoran ruminants are now only represented by the family Tragulidae. However, the early ruminant fossil record includes various groups of extinct hornless ruminants, first appearing in the middle Eocene (~45 Ma) and later diversifying in the Oligocene, prior to the expansion of pecorans in the Neogene and Quaternary (Métais & Vislobokova, 2007; Vislobokova, 2001).

The evolution and systematics of early ruminants remain enigmatic. Previous attempts to resolve the phylogenetic relationships of early ruminants have generated highly varied results at both generic and species levels (e.g., Geraads et al., 1987; Guo et al., 1999, 2000; Janis, 1987; Mennecart & Métais, 2015; Métais et al., 2001; Métais, 2006; Scott & Janis, 1992; Webb & Taylor, 1980), with the relatively poor quality of the fossil record presenting a major challenge. Better understanding the evolution of early ruminants, particularly against the backdrop of climatic and environmental changes during the Eocene–Oligocene transition, relies on the continued discovery of well-preserved fossil materials.

In Asia, previously reported early Oligocene ruminant fossils have primarily originated from Mongolia and Kazakhstan (Métais & Vislobokova, 2007; Vislobokova & Daxner-Höck, 2002). Herein, we report new dental materials from the Saint Jacques-Qianlishan area, western Nei Mongol, China. Re-exploration of the classic Oligocene site of Saint Jacques has yielded abundant fossil mammal materials, among which four species of the stem ruminant *Lophiomeryx* have recently been reported (Wang, B., Wang, et al., 2023; Wang, B., Zhang, et al., 2023). The materials described in the present study were identified as three additional genera of ruminants: *Praetragulus*, *Gobiomeryx* and *Paragelocus*. *Praetragulus* and *Gobiomeryx* are primarily known from the late Eocene to early Oligocene of Mongolia and China (Guo et al., 1999; Vislobokova, 1998; 2001; Wang, B.-Y. et al., 1981). *Paragelocus* is known from the early Oligocene of Europe and Mongolia (Schlosser, 1902; Vislobokova & Daxner-Höck, 2002). None of the three genera is diverse at the species level. There are two previously recognized species of *Praetragulus*, *Gobiomeryx* and *Paragelocus* are monotypic. This study

Corresponding author. Email: zhangzhaoqun@ivpp.ac.cn

Published online 19 Sep 2025

describes new dental specimens from Nei Mongol and posits the phylogenetic relationships of the reported taxa. It also examines how these fossils contribute to understanding the diversity and systematics of early ruminants in the Oligocene of Asia.

Materials and methods

All new materials are housed at the Institute of Vertebrate Paleontology and Paleoanthropology of the Chinese Academy of Sciences in Beijing. The materials include 115 dental specimens collected between 2012 and 2023 from Saint Jacques, Nei Mongol Autonomous Region, China, supplemented by two specimens from a nearby locality, Qianlishan. Saint Jacques is located on the northwestern margin of the Ordos Plateau near the town of Balagong, Hanggin Banner, Ordos City and Qianlishan is approximately 20 km to the south of Saint Jacques (Fig. 1A, B). The Saint Jacques specimens were excavated from fossiliferous blocks A, D, F, J, N, Q, R and T, and their stratigraphical levels are reported with reference to the composite stratigraphical column of Saint Jacques, which is divided into 12 litho-units (Wang, B., Zhang, et al. 2023; Fig. 1C, Supplemental Tables S1–S3). Specimens attributed to *Praetragulus* span litho-units 5–8, although the vast majority of the specimens are from litho-unit 7, a sandstone layer. Specimens attributed to *Gobiomeryx* occur in litho-unit 7 only, while those attributed to *Paragelocus* are found in litho-units 5 through 7. Small-mammal biostratigraphical analysis and correlation with the palaeomagnetic dated Ulantatal sequence (Wasiljeff & Zhang., 2022) suggest an Early Oligocene age (34–28 Ma) of these units (Wang, B., Zhang, et al. 2023). The two specimens from Qianlishan were collected from horizon no. 17, top of the Wulanbulage Formation (Wang, B.-Y. et al., 1981).

To investigate the phylogenetic relationships of the ruminants from Saint Jacques-Qianlishan, we generated a matrix of 52 morphological characters with 30 taxa. The character matrix was mainly derived from Mennecart and Métais (2015) (37 dental and postcranial characters, 11 species), with additional characters and species that better suit the taxonomic and geographical scope of this study (Supplemental Appendix A). *Diacodexis pakistanensis*, one of the most primitive artiodactyls (Kumar et al., 2010; Thewissen et al., 1983; Thewissen & Hussain, 1990), was selected as the outgroup. Two other non-ruminant artiodactyls from the Eocene of Asia, *Gobiohyus orientalis* and *Haqueina haichinensis*, were also included (Coombs & Coombs, 1977; Ducrocq, 2019; Matthew & Granger, 1925a; Vislobokova, 2004; Wang, B. et al., 2025). Character coding of ruminant species was based on our own observation of museum specimens and on information from published sources (e.g., Becker et al., 2004; Bouvrain et al., 1986; Boyd & Welsh, 2014; Brunet & Sudre, 1987; Colbert, 1941; Dong et al., 2003; Ducrocq et al., 2021, 2023; Janis & Scott, 1987; Korth & Diamond, 2002; Mennecart, 2012, 2015; Mennecart et al., 2011; Métais et al., 2009, 2017; Morales et al., 2003; Sánchez & Morales, 2008; Sudre, 1984). Character matrix was assembled in Mesquite v.3.81 (Mesquite Project Team, 2023). The character list, data matrix and taxon-specific references are presented in the Supplemental Appendices.

The phylogenetic analysis was performed in TNT v.1.6 (Goloboff & Morales, 2023), using a heuristic search with tree bisection-reconnection (TBR) branch swapping and 1000 replicates of the random addition sequence, saving 100 trees per replication and collapsing trees after the search. All characters are equally weighted and unordered. Gaps are treated as 'missing'. Bremer support values were calculated after 1000 replicates using the built-in function.

Anatomical nomenclature

Dental nomenclature follows Bärmann & Rössner (2011).

Institutional abbreviations

AMNH, American Museum of Natural History, New York, NY, USA; **IVPP**, Institute of Vertebrate Paleontology and Paleoanthropology, Beijing, China; **NHMW**, Museum of Natural History of Vienna, Vienna, Austria; **PIN**, Paleontological Institute of Russian Academy of Sciences, Moscow, Russia.

Anatomical abbreviations

dp, lower deciduous premolar; **M**, upper molar; **m**, lower molar; **P**, upper premolar; **p**, lower premolar.

Systematic palaeontology

Order **Artiodactyla** Owen, 1848
Suborder **Ruminantia** Scopoli, 1777
Genus ***Praetragulus*** Vislobokova, 1998

Type species. *Praetragulus electus* Vislobokova, 1998

Included species. *Praetragulus gobiae* Matthew & Granger, 1925b

Praetragulus ordosianus sp. nov.
Supplemental Table S1, Fig. 2

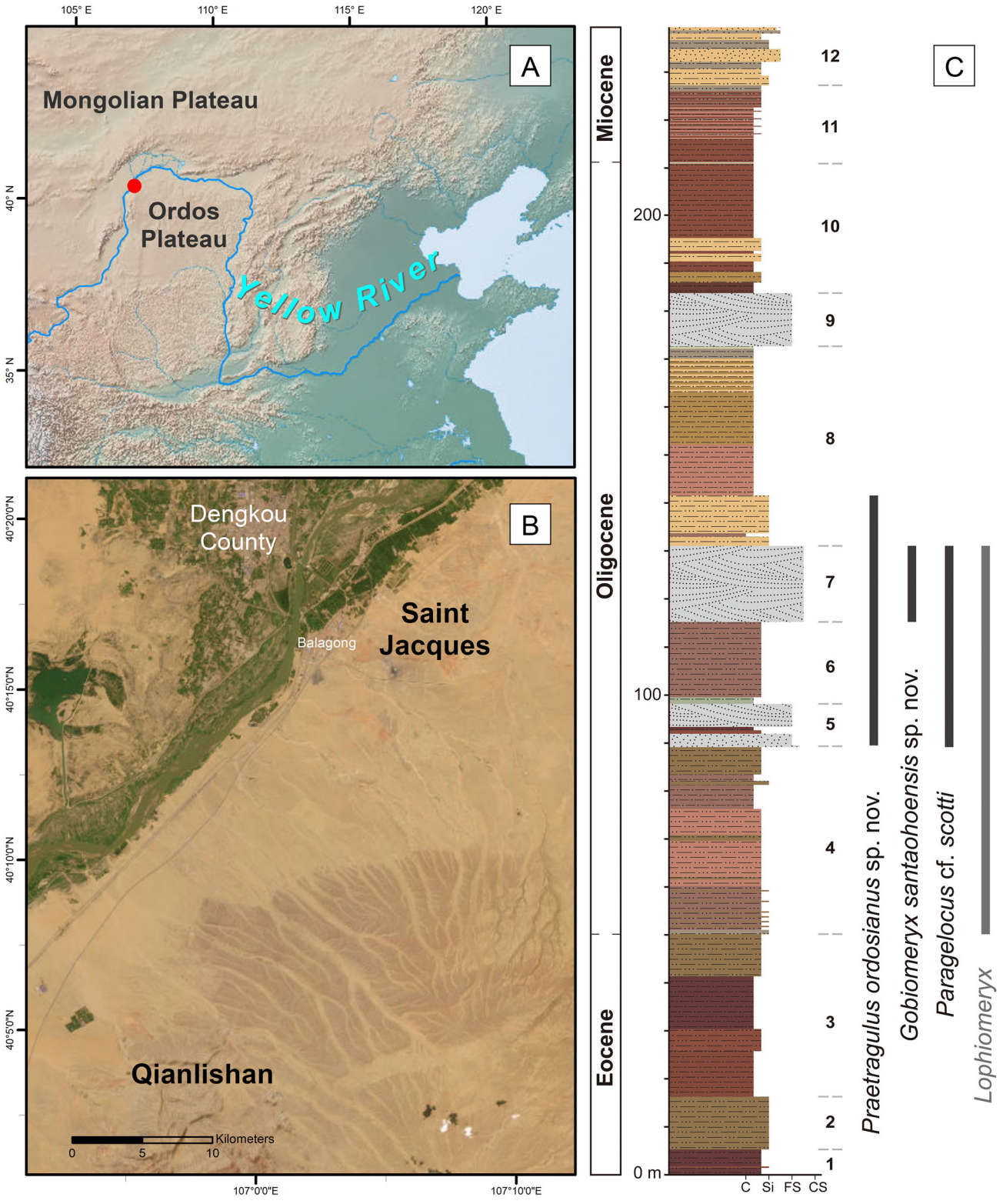

Figure 1. Location and stratigraphy of the study area. **A,** The Saint Jacques-Qianlishan area (red circle) sits on the north-western margin of the Ordos plateau, along the Yellow River. **B,** Most of the new materials were collected from Saint Jacques; two additional specimens were collected from a nearby site, Qianlishan. **C,** The Eocene to Miocene strata at Saint Jacques are divided into 12 lithostratigraphical units (Wang, B., Zhang, et al. 2023) and ruminant taxa have different stratigraphical ranges. See Wang, B., Wang, et al. (2023) for details about *Lophiomeryx*.

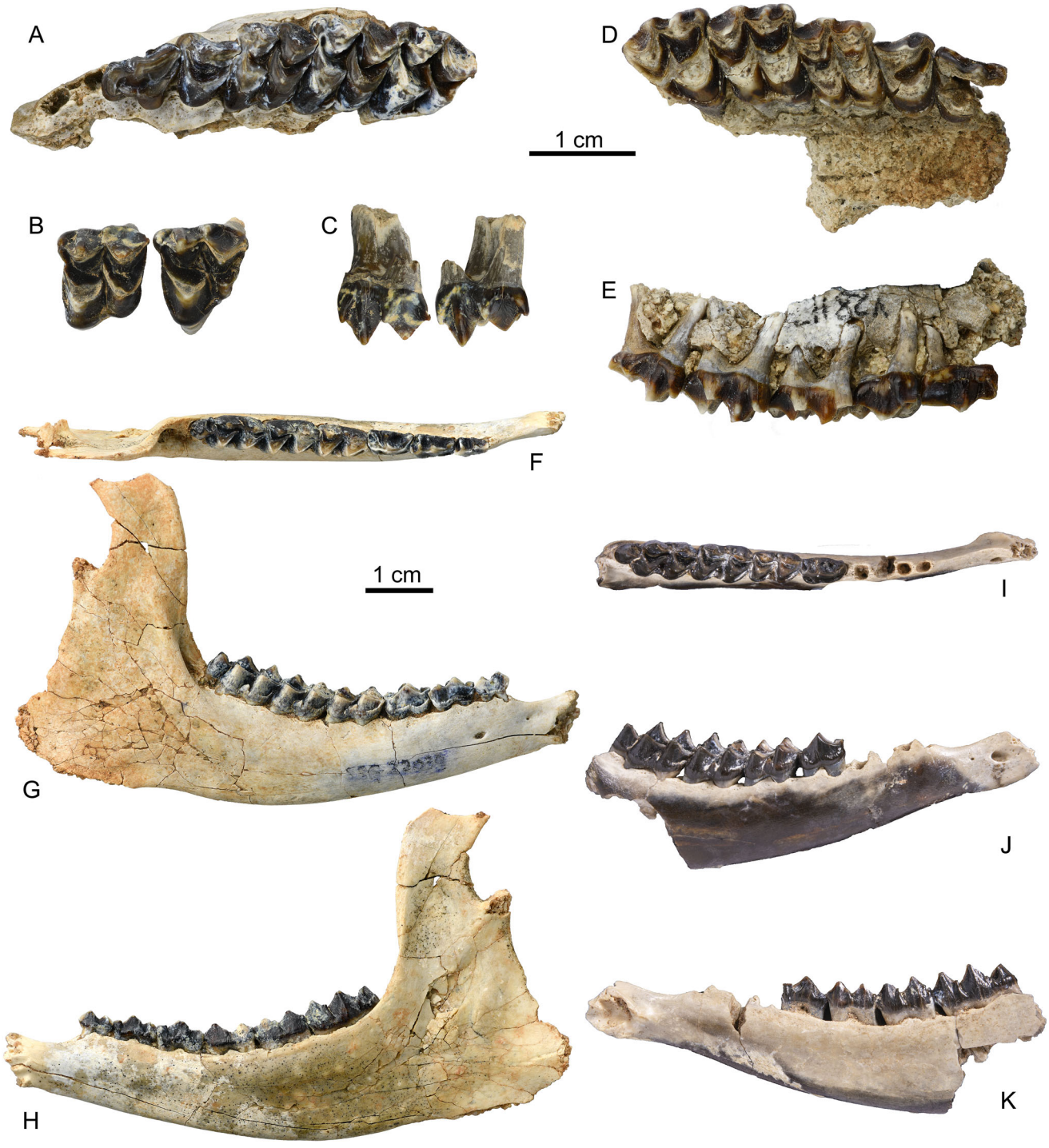

Figure 2. Selected specimens of *Praetragulus ordosianus* sp. nov. from Saint Jacques. **A,** IVPP V28130 (paratype), left maxilla with P3–M3. IVPP V28128–V28129, left M2–M3 in **B,** occlusal and **C,** labial views. IVPP V28117, right maxilla with P3–M3 in **D,** occlusal and **E,** labial views. IVPP V33261 (holotype), right mandible with p2–m3 in **F,** occlusal; **G,** labial; and **H,** lingual views. IVPP V28135, right mandible with p4–m3 in **I,** occlusal; **J,** labial; and **K,** lingual views. Scale bars differ for upper (A–E) and lower teeth (F–K).

Holotype. IVPP V33261, lower jaw with right p2–m3.

Paratype. IVPP V28130, upper jaw with right P3–M3.

Included specimens. Upper jaw with left P3–M3: V28117. P4: V28118. Four M1: V28119, V28122, V28124 V28131. Five M2: V28120, V28125–V28128. Five M3: V28121, V28123, V28129, V28132, V28133. Lower jaws, with p2–p4: V28150; with p3–p4: V28153; with p4: V28181; with p4–m1: V28147, V28156; with p4–m2: V28155; with p4–m3: V28180, V28135; with m1: V28143, V28157; with m1–m2: V28138; with m1–m3: V28140, V28158, V28167, V28182, V28186; with m2: V28162, V28163, V28168; with m2–m3: V28141; with m3: V28151, V28161. Three p3: V28145, V28173–28174. Eight p4: V28134, V28136, V28139, V28175–28177, V28181, V28188. Thirteen m1: V28137, V28142, V28159–28160, V28165, V28171, V28178, V28183, V28190–28194. Eight m2: V28148, V28154, V28166, V28169–28170, V28179, V28187, V28195. Six m3: V28144, V28146, V28149, V28152, V28164, V28172.

Locality, horizon and age. Saint Jacques, Nei Mongol, China; litho-units 5–8; late Early Oligocene.

Etymology. The species name refers to the Ordos plateau, where the type locality is located.

Diagnosis. Moderately well-developed parastyle, mesostyle and anterior rib on upper molar; parastyle anteroposteriorly compressed; postprotocrista extends posterolabially and without bifurcation; weakly developed bifurcation of the prematacondecrista; well-developed anterior, lingual and posterior cingula connecting with each other; metaconule highly reduced on M3; lower premolar row shorter than lower molar row; no p1; no diastema between p2 and p3; p4 with well-developed mesolingual conid and posterior cristid, labial cingulid, and a small pit in the posterolabial corner; well-developed anterior and posterior cingulids, metastylid and ectostylid on lower molars; short posthypoconulidcristid on m3, hypotalonid basin opens to the lingual side.

Differential diagnosis. Differs from *Praetragulus electus* by longer lower premolar row, longer posterolingual cristid on p4, and better developed ectostylid on lower molars. Differs from *Praetragulus gobiae* by less prominent mesostyle and the presence of premetaconulecrista bifurcation on upper molars, longer lower premolar row, posterolingual conid on p4, and better-developed ectostylid, metastylid and postentocristid on lower molars.

Description. Abundant dental materials are recovered from Saint Jacques, including maxillae and mandibles with complete cheek tooth rows. The cheek teeth are brachydont. In lateral view, the upper and lower cheek tooth rows slightly curve downwards.

Mandible. The c–p2 diastema is roughly as long as p2–p3, as approximated by the alveoli. The mandibular body is slender and markedly higher under the posterior cheek teeth than the anterior check teeth. The ventral border of the mandibular body is curved downwards. The anterior mental foramen is large, placed at the level of the anterior c–p2 diastema. A small posterior mental foramen is present, situated at the level of the middle of the c–p2 diastema. The symphysis extends to the level of the anterior mental foramen. There are three relatively small alveoli preserved at the anterior end of the mandible. The size of the canine alveolus is similar to that of the last incisor (i3). The i2 alveolus is smaller. Additionally, the lateral half of the i1 alveolus is present, showing that i1 is markedly larger than other incisors. The orientation of these alveoli suggests that the incisors and the canine are procumbent. The angular process projects downward and backward, with a broad and shallow masseteric fossa. The coronoid process is high and wide between its anterior and posterior borders. It is generally perpendicular to the mandibular body but curves backward towards the top. The mandibular notch is shallow and narrow. The mandibular condyle is at the mid-height of the ramus and has a short neck. On the lingual side of the mandible, the pterygoid fossa is broad, and the mandibular foramen is at the same height as the check teeth.

Upper dentition. The labial outline of the upper cheek tooth row curves outward, while the lingual outline is almost straight. No P2 specimen is collected so far, although the P2 alveolus is preserved on IVPP V28130. On P3, the parastyle is crest-like and extends lingually, the anterior rib and metastyle are moderately developed, and the lingual cone is weakly crescent-shaped. The labial side of P3 is oblique to the tooth row axis, while the lingual side is generally parallel to this axis. P4 is wider and shorter than P3, with a better-developed lingual cone surrounded at the base by thin yet distinct cingulum. The parastyle on P4 is smaller than that of P3 but is slightly bigger and more rounded than those of the molars. The lingual cone is crescentic and connected to the labial wall of P4 by the anterolingual crista and posterolingual crista.

The upper molars are similar in overall morphology, longer on the labial side than the lingual side and wider at the anterior lobe than the posterior lobe. The parastyle, anterior rib and mesostyle are moderately developed. The parastyle is slightly compressed anteroposteriorly. The mesostyle widens toward its base, connecting with the bottom of the anterior rib in some cases. The anterior rib is well-developed and bends

anteriorly. The posterior rib is absent. The metastyle is rather reduced on M1 but it is better developed on M3. The postprotocrista is relatively short, extending posterolabially to join the premetaconulecrista at the middle. The premetaconulecrista extends toward the paracone-metacone junction but does not reach it. In relatively unworn teeth, it can be shown that the posterior end of the postparacrista is situated lower than the premetacrista, and the posterior end of the postprotocrista is lower than the premetaconulecrista. The premetaconulecrista bifurcation is present but very thin. The postmetaconulecrista is long and connects with the metastyle. The anterior, lingual and posterior cingula are well-developed, together wrapping around the base of the protocone and the metaconule. A small entostyle is present on M1 and M2 but becomes much smaller to absent on M3. The metaconule is slightly smaller than the protocone on M1 and M2, but much smaller on M3, giving M3 an overall triangular occlusal outline.

Lower dentition. The absence of the alveolus for p1 on the type specimen implies that p1 is evolutionarily lost. On p2, the anterior conid and the mesolingual conid are barely developed; the mesolabial conid and the posterolingual conid are relatively high, thus the tooth has an almost bicusped profile in lateral view; the anterolabial and posterolabial cristids, transverse cristid and posterolingual cristid are developed; the posterolabial conid is slightly lower than the posterolingual; the back valley is wide open posteriorly. The posterior end of p2 is notably wider than the anterior end of it. The proportions of p3 are similar to those of p2, but p3 is larger. On p3, the anterior conid is well developed and extends anterolingually; the mesolabial conid is prominent; the transverse cristid extends posterolabially from the mesolabial conid to a lower, weaker mesolingual conid; the posterior cristid extends primarily lingually; the posterolabial conid is present; the back valley is largely open posterolingually. Compared to p3, p4 is wider and slightly shorter. The posterolabial conid of p4 is at the midpoint of the tooth. The mesolingual conid and posterior stylid are well developed, and the posterior cristid is posterolingually oriented. The transverse cristid is slightly 'V'-shaped and points posteriorly. The back valley of p4 becomes enclosed when the tooth is worn down. A small pit, enclosed by the labial wall and the cingulid, is present in the posterolabial corner of p4. Labial cingulids are present on all the premolars, being weak on p2 but increasingly developed toward p4.

The lower molars have mediolaterally compressed lingual cuspids (metaconid and entoconid) and crescent-shaped labial cuspids (protoconid and hypoconid). The lingual cuspids are higher than the labial cuspids. The metastylid is well developed. The ectostylid relatively tall and conical, largest on m1 and slightly smaller on m3. The cross-section of the ectostylid is oval in shape, with a long axis perpendicular to the prehypocristid. The premetacristid and the preprotocristid converge anteriorly, gently connecting at the base at the anterior margin of the teeth, thus the trigonid basin only appears closed anteriorly when the tooth is heavily worn. The postentocristid is well developed but does not connect fully with the posthypocristid which extends to the lingual side, thus the talonid basin has a small posterolingual opening and only becomes closed when the tooth is heavily worn. The preentocristid joins the postprotocristid–postmetacristid junction anteriorly. The prehypocristid is lower than the former three and does not become confluent with them until the tooth is worn to its level. The anterior cingulid is developed, extending from the lingual side all the way to the labial side around the anterior margin of the tooth. The posterior cingulid is less developed than the anterior cingulid. On m3, there is a rather small posterior ectostylid, which is absent in some specimens. The third lobe of m3 is largely unicusped; the hypoconulid is situated at the posterior margin of m3. The prehypoconulidcristid connects anteriorly with the posthypocristid. The posthypoconulidcristid is short, leaving the hypotalonid basin somewhat open to the lingual side. There is a small, blunt tubercle at the base of the postentocristid, which may be the entostylid or a rudimentary entoconulid.

Genus ***Gobiomeryx*** Trofimov, 1957

Type species. *Gobiomeryx dubius* Trofimov, 1957

Gobiomeryx santaohoensis sp. nov.

Supplemental Table S2, Fig. 3

Etymology. The species suffix is derived from the original name of Saint Jacques, San-tao-ho.

Holotype. IVPP V28222, right mandible with p1, uneruptedp2 and p3 and dp4–m3.

Included specimens. Four partial mandibles: IVPP V28223, left mandible with p2–m3; V28224, right mandible with m2–m3; V28225, left mandible with m3; V28228, left mandible with dp4–m1. Two m2: V28229, V28231. Four m3: V28226, V28227, V28230, V28232.

Locality, horizon and age. Saint Jacques, Nei Mongol, China; litho-unit 7; late Early Oligocene.

Diagnosis. Mandibular body widened labially at its mid height; p1 single cusped, no p1–p2 diastema; p4 with enclosed back valley; small posterolingual opening in the talonid basin of lower molars due to relatively short postentocristid; metastylid and ectostylid present;

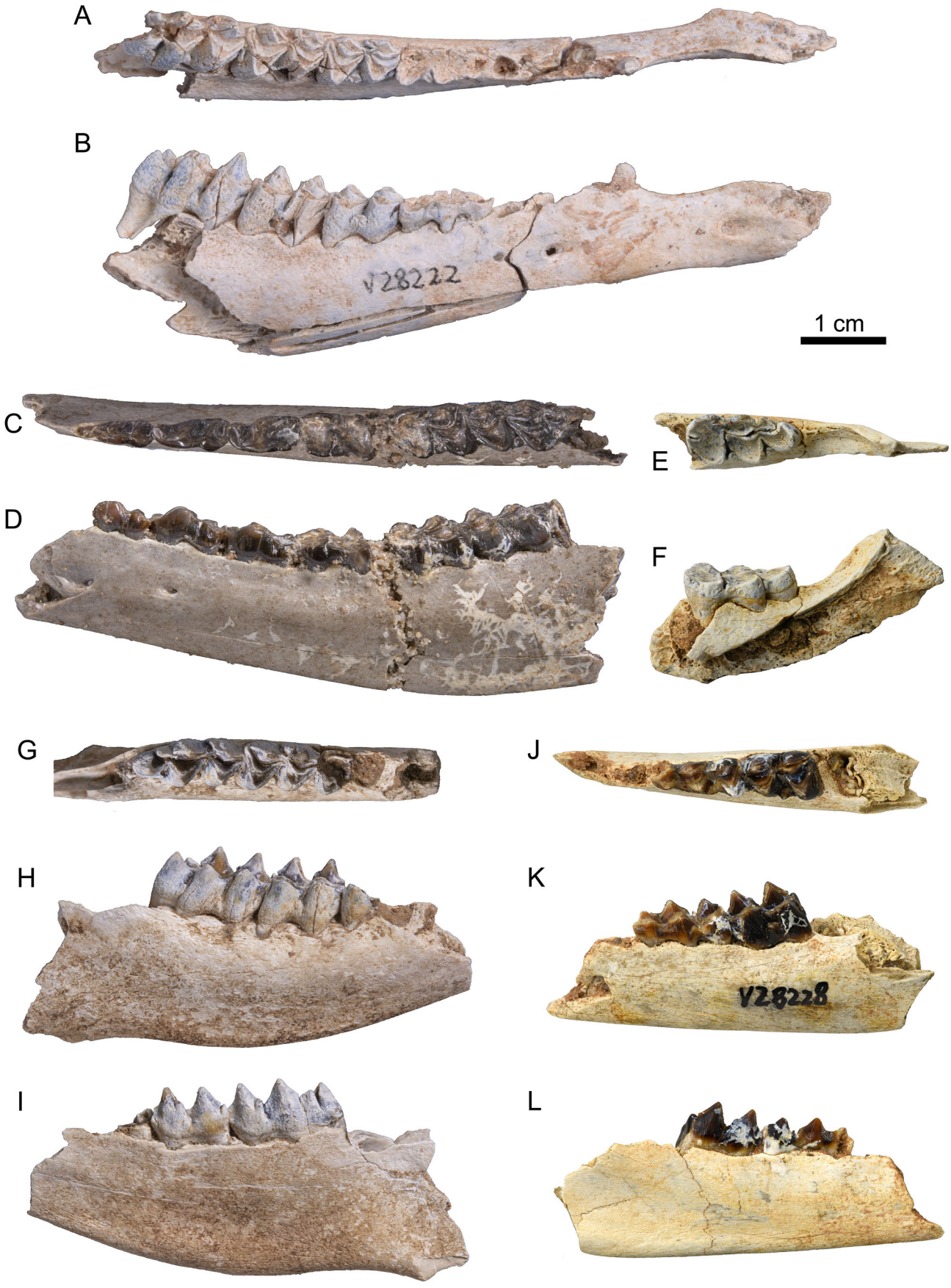
A
B
V28222
1 cm
C
E
D
F
G
J
H
K
V28228
I
L

posterior ectostylid and prominent entoconulid present on m3; hypotalonid basin on m3 opens anteriorly.

Differential diagnosis. Differs from *Gobiomeryx dubius* by its larger size, increased crown height, and better-developed entoconulid.

Description. The new samples include fragmentary mandibles and isolated lower molars. No upper dentition has been collected so far.

Mandible. The mandibular body is wider at the mid-height. The depth of the mandibular body is greater under the lower molars than premolars. The ventral border of the mandibular body has a flexure point at the level of m2–m3. The type specimen (IVPP V28222) shows a lower dental formula of 3/1/4/3, although no incisors or canine is preserved. The alveoli of i2, i3 and c are comparable in size, while the i1 alveolus is markedly larger. The orientation of these alveoli suggests that the incisors and the canine are procumbent. The length of the c-p1 diastema is roughly equivalent to p1–p3. There is no diastema between p1 and p2. There are two mental foramina. The anterior mental foramen is larger, situated below the anterior part of the diastema. The posterior mental foramen is below the anterior lobe of p3. The specimen displays the replacement sequence of lower cheek teeth. It retains a slightly worn p1, unerupted p2 and p3, highly worn dp4, and fully erupted molars with decreasing level of wear from m1 to m3. This indicates that dp4 is the last deciduous tooth to be replaced by a permanent tooth, and this replacement occurs sometime after all molars are fully erupted.

Lower dentition. The retained p1 is single-rooted and single-cusped. Both p2 and p3 are long and narrow. On p2, there is weak anterior conid, prominent mesolabial conid, relatively low posterolingual conid and posterolabial conid, posteriorly oriented transverse cristid, short posterior cristid and weak posterior stylid. The posterolabial conid is conical, giving the posterolabial corner of the tooth a rounded outline in occlusal view. The posterior valley is open to the lingual side. Morphologically similar to p2, p3 differs from p2 by its larger size, better-developed anterior conid with anterolingual extension, posterolingually oriented transverse cristid, longer posterolingual cristid and better-developed posterior stylid that extends to the lingual side of the tooth. Slightly shorter and wider than p3, p4 has crest-like anterior conid, well-developed mesolingual conid, posterolingual conid, posterolabial conid and posterior stylid. The transverse cristid on p4 is 'V'-shaped. The mesolingual conid slightly stretches anteroposteriorly, forming a posterolingual cristid. The posterior cristid is thin and long, extending posterolingually from the mesolabial conid and ends at the posterolingual corner of the tooth; the back valley is largely enclosed. The posterolabial conid on p4 does not have a bulbous labial surface, and so the tooth has a more rectangular outline compared to p2 and p3. There is no cingulid on the lower premolars.

On the lower molars, both the premetacristid and preprotocristid extend anteriorly; however, they are not connected, leaving the trigonid basin slightly open anteriorly. On m1 and m2, the posthypocristid is long, extending to the lingual side but not connecting with the postentocristid, thus the talonid basin has a small lingual opening. On m3, the posthypocristid is shorter, and the talonid basin is open posteriorly and connected with the hypotalonid basin. The ectostylid and metastylid on the lower molars are well-developed. The ectostylid is slightly smaller on m3 than on m1. The premetacristid and the preentocristid both extend anteriorly, parallel to the long axis of the mandibular body, while the postmetacristid and postentocristid (except for m3 postentocristid) are slightly oblique to it. On the third lobe of m3, a posterior ectostylid is present, and there is a prominent entoconulid, placed at the posterior end of the postentocristid. The posthypoconulidcristid is short and does not connect with the entoconulid, thus leaving a small posterolingual opening to the hypotalonid basin. Anterior and posterior cingulids are present on the lower molars; labial cingulids are absent.

Genus ***Paragelocus*** Schlosser, 1902

Type species. *Paragelocus scotti* Schlosser, 1902

Paragelocus* cf. *scotti

Supplemental Table S3, Figs 4, 5

Referred specimens. Three M1: IVPP V28197, V28198, V28201. Three M2: V28199, V28202–V28203. Five M3: V28196, V28200, V28204, V28205, V28206. Seven p4: V28207–V28208, V28213–V28215, V28217, V28221. Nine partial mandibles: with p2–p4, V28209, V28211; with p2–m2, V28219; with p3–p4, V28212,

Figure 3. Selected specimens of *Gobiomeryx santaohoensis* sp. nov. from Saint Jacques. IVPP V28222 (holotype), right mandible with p1, unerupted p2–p3 and dp4–m3 in **A,** occlusal; and **B,** labial views. IVPP V28223, left p2–m3 in **C,** occlusal; and **D,** labial views. IVPP V28225, partial left mandible with m3 in **E,** occlusal; and **F,** labial views. IVPP V28224, partial right mandible with m2–m3 in **G,** occlusal; **H,** labial; and **I,** lingual views. IVPP V28228, left dp4–m1 in **J,** occlusal; **K,** labial; and **L,** lingual views.

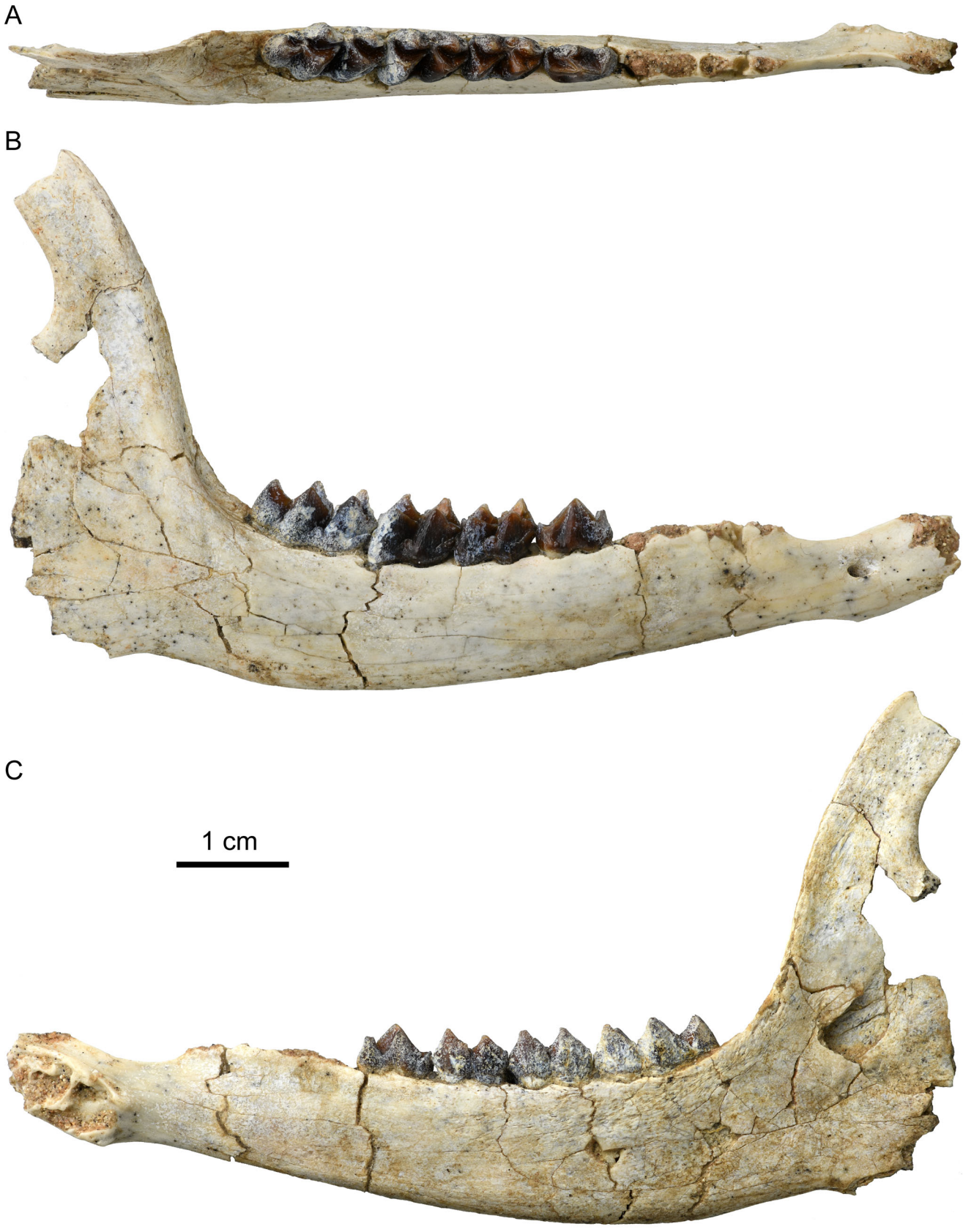

Figure 4. Right mandible with p4–m3 (IVPP V33262) attributed to *Paragelocus* cf. *scotti*, in **A,** occlusal; **B,** labial; and **C,** lingual views.

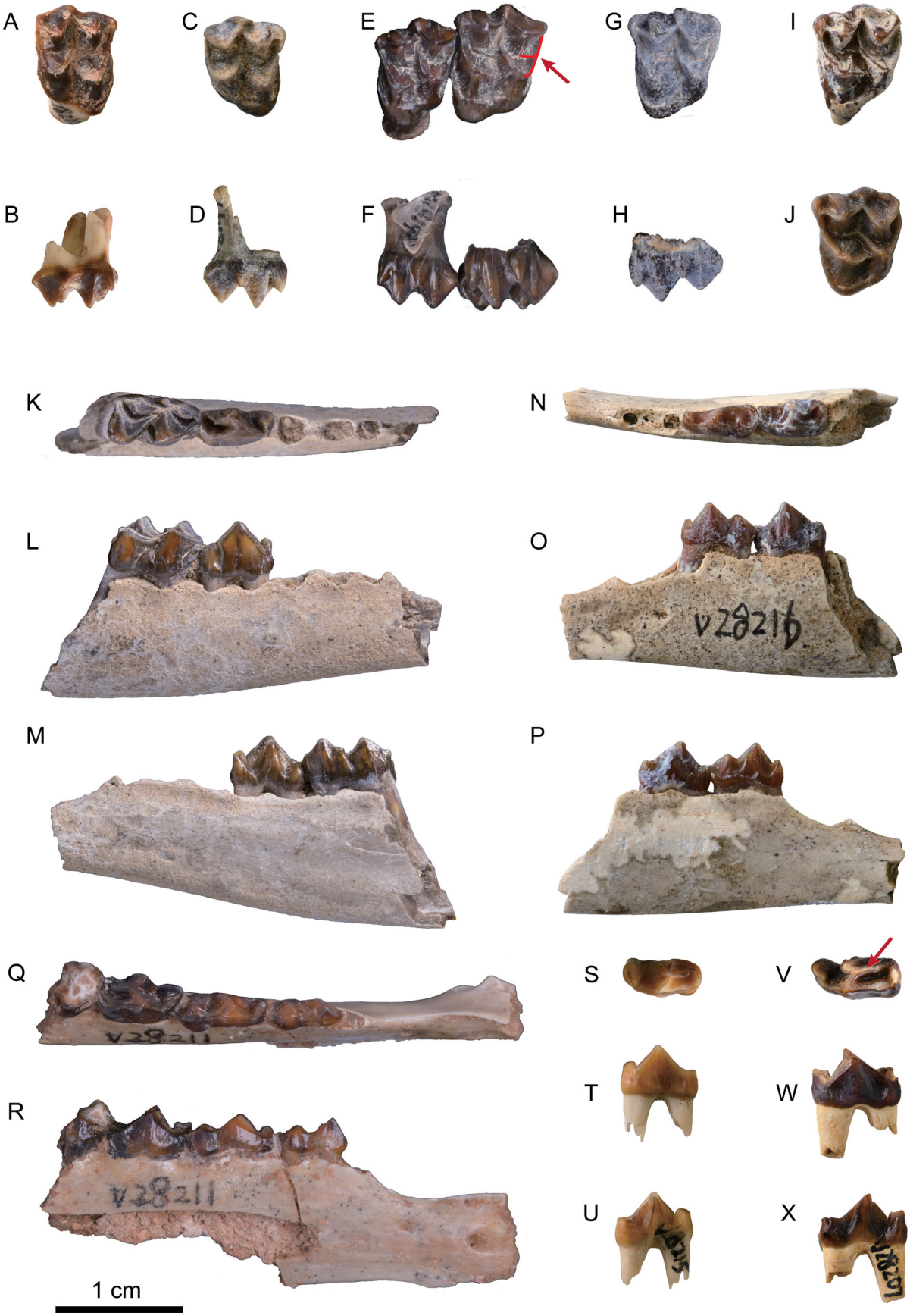
A
C
E
G
I
B
D
F
H
J
K
N
L
O
V28216
M
P
Q
V28211
S
V
T
W
R
V28211
U
X
1 cm

V28216; with p4–m1, V28218, V28220; with p4–m3, V33262; with m2, V28210.

Locality, horizon and age. Saint Jacques, Nei Mongol, China; litho-units 5–7; late Early Oligocene. Qianlishan, Nei Mongol, China; horizon no. 17, late Early Oligocene.

Description. The materials include isolated teeth as well as mandibles.

Mandible. The mandible is slender and thin. The height of the mandibular body does not vary much under the cheek teeth. The ventral border of the mandible is slightly curved. The diastema between canine and p1 is roughly as long as p1–p3. There is no diastema between p1 and p2. The anterior mental foramen is under the c–p1 diastema. The anterior border of the ramus and the tooth row axis form an angle slightly greater than 90°. The coronoid process is high and wide. It curves slightly backward toward its top. The mandibular foramen is visible on the lingual side, slightly higher than the level of the cheek teeth.

Upper dentition. The upper molars are brachydont. The parastyle has a rounded anterior outline. The mesostyle is strong and widens toward its base, forming a triangular outline in labial view. The metastyle is small. The anterior rib is well developed and bends anteriorly. The posterior rib is weak to absent. The metaconule is comparable in size to the protocone on M1 and M2 but is highly reduced on M3. The postprotocrista is short and straight, extending posteriorly. The premetaconulecrista extends to the paracone–metacone junction but does not reach it. The postprotocrista bifurcation and the premetaconulecrista bifurcation are present. In most specimens, two additional cristids are present in the posterior fossa. The first one is blunt and extends labially from the metaconule, paralleling the postprotocrista bifurcation; the other is low and short, connecting the lingual base of the metacone and the middle of the postmetaconule, forming what appears to be postmetaconule bifurcation. On M3, there is a small cusp-like bump on the preprotocrista near the protocone, which appears to be an incipient paraconule. The anterior and lingual cingula are strong and connected. The lingual cingulum at the base of the protocone is particularly thick and shelf-like, giving the protocone a prominent lingual extension and making the anterior lobe much wider than the posterior lobe. The posterior cingulum is weak on M1 and M2 and absent on M3.

Lower dentition. The single-rooted p1 alveolus is present on some specimens, although no tooth is preserved, but absent on others. On p2, there is weak anterior conid, tall mesolabial conid, and no mesolingual conid. The transverse cristid is short and posterolingually oriented. The posterolingual and posterolabial conids appear to be both present although not well differentiated from each other. On p3, the anterior conid is small but distinct, crest-like. The mesolabial conid is tall. The transverse cristid extends posterolingually. The mesolingual conid is absent; the posterolingual conid and posterolabial conid are present. The anterior conid of p4 is also crest-like. The mesolabial conid of p4 sits at the mid-length of the tooth, more posteriorly placed compared to its location on p2 and p3. The p4 mesolingual conid is well developed, with a short, variably present posterolingual cristid and no anterolingual cristid. The transverse cristid bends posteriorly to form a 'V'-shape in occlusal view, connected posteriorly with the posterior stylid by a ridge-like longitudinal cristid, which is straight and tall in some specimens but is thin and bends labially in other specimens. The posterolingual conid and posterior cristid are absent. Consequently, the posterior valley and back valley of p4 are fully connected, forming a deep, enclosed basin. The premolars lack cingulids, but there is a small pit on the labial surface of p4 below the posterolabial conid, which is visible in labial and occlusal views.

On the lower molars, the metaconid and the entoconid have pillar-like lingual surfaces. The ectostylid and the metastylid are present. The preprotocristid is interrupted by a small, incipient cuspid at its midpoint, and correspondingly there is a shallow notch in the labial side of the trigonid basin. The premetacristid and the preprotocristid are not fully connected anteriorly, thus the trigonid basin appears open anteriorly but closes as the tooth wears down. The posthypocristid extends to the lingual side and connects with the postentocristid. The anterior and posterior cingulids are present, with thick labial extension. The third lobe of m3 is unicusped. The hypoconulid is situated at the posterior margin of m3. The prehypoconulidcristid connects anteriorly with the posthypocristid. The posthypoconulidcristid is short, leaving the hypotalonid basin somewhat open to the lingual side. There is a small, blunt tubercle at the base of the postentocristid.

Figure 5. Selected specimens of *Paragelocus* cf. *scotti* from Saint Jacques. **A, B,** right M2 (IVPP V28202); **C, D,** right M1 (IVPP V28197); **E, F,** left M1–M2 (IVPP V28198–V28199); **G, H,** left M3 (IVPP V28204); **I,** left M3 (IVPP V28206); **J,** left M3 (IVPP V28200); **K–M,** right mandible with p4–m1 (IVPP V28220); **N–P,** left mandible with p3–p4 (IVPP V28216); **Q, R,** right mandible with p1 alveolus, p2–p4 and partial m1 (IVPP V28211); **S–U,** left p4 (IVPP V28215); **V–X,** left p4 (IVPP V28207). A, C, E, G, I, J, K, N, Q, S and V in occlusal view; B, D, F, H, L, O, R, T and W in labial view; M, P, U and X in lingual view. The postmetaconulecrista bifurcation on upper molar and the longitudinal cristid on lower p4 are marked with arrows in E and V, respectively.

Remarks. The special p4 morphology observed on the referred specimens also resembles that of *Paragelocus scotti* from the early Oligocene of Europe, which is the only member of its genus, characterized by its very strong upper molar cingulum, anteriorly rounded parastyle, short and posteriorly oriented postprotocrista, and a small paraconule (Schlosser, 1902). However, the referred specimens are larger than *P. scotti* (Supplemental Table S3). The specimens have M3 morphology similar to *Paragelocus* aff. *scotti* described by Vislobokova and Daxner-Höck (2002), but the p3 entocristid is not as developed as in the latter (NHMW 2001z0090/0003). Based on p4 and upper molar morphology, we attribute the new specimens to *Paragelocus* cf. *P. scotti*.

These specimens exhibit a unique combination of features. In the upper molars, there is a short, thin crista connecting the base of the metacone to the middle of the postmetaconulecrista. Its morphology and orientation parallel the premetaconulecrista bifurcation, thus we call it postmetaconulecrista bifurcation, which to our knowledge is absent in other ruminant genera. Lower premolars are peculiar in two aspects. First, p1 is variably present. Second, p4 exhibits a range of size, the posterolingual cristid is variably present, and the longitudinal cristid

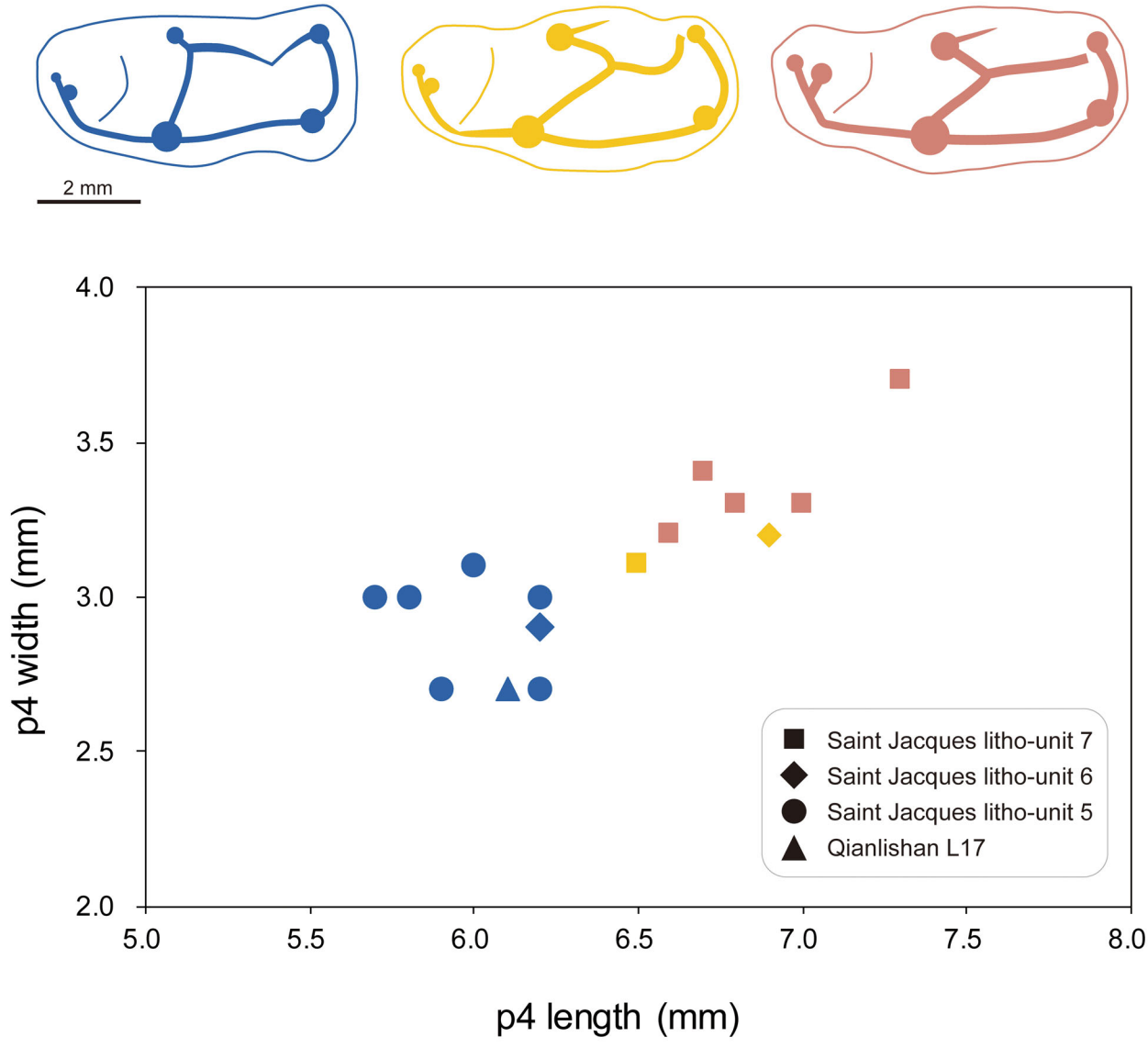

Figure 6. Variation in the p4 morphology of *Paragelocus* cf. *scotti* identified in this study. Illustrations of three representative p4 morphologies are based on IVPP specimens V28209 (blue), V28213 (yellow) and V28208 (pink). The general changes from older to younger specimens include larger size, presence of the posterolingual cristid, thickening and straightening of a longitudinal cristid which extends posteriorly from the transverse cristid, and better developed anterior bifurcation.

exhibits two main states. Generally speaking, specimens from litho-unit 5 are smaller, lack posterolingual cristid, and have a thin, wiggly longitudinal cristid which appears to be formed by a posterior extension of the transverse cristid and an anterior extension of the posterior stylid; meanwhile, specimens from litho-unit 7 are larger, with variably developed posterolingual cristid present, and with a tall, straight longitudinal cristid that is fully developed (Fig. 6). An intermediate state also exists, although only displayed in two specimens, with the presence of posterolingual cristid associated with a weak, wiggly longitudinal cristid. This (partial) dichotomy suggests a possibility of two taxa. However, the two p4 states are not linked to either presence or absence of p1 (Supplemental Table S4), and we do not observe a comparable level of variation in the morphology of upper molar specimens. Therefore, we tentatively attribute these specimens to the same taxon. A plausible explanation is that, from litho-unit 5 to litho-unit 7, we observe a transition in p4 morphology within the same lineage, in which p1 has become an unstable characteristic, present in some individuals but not in others.

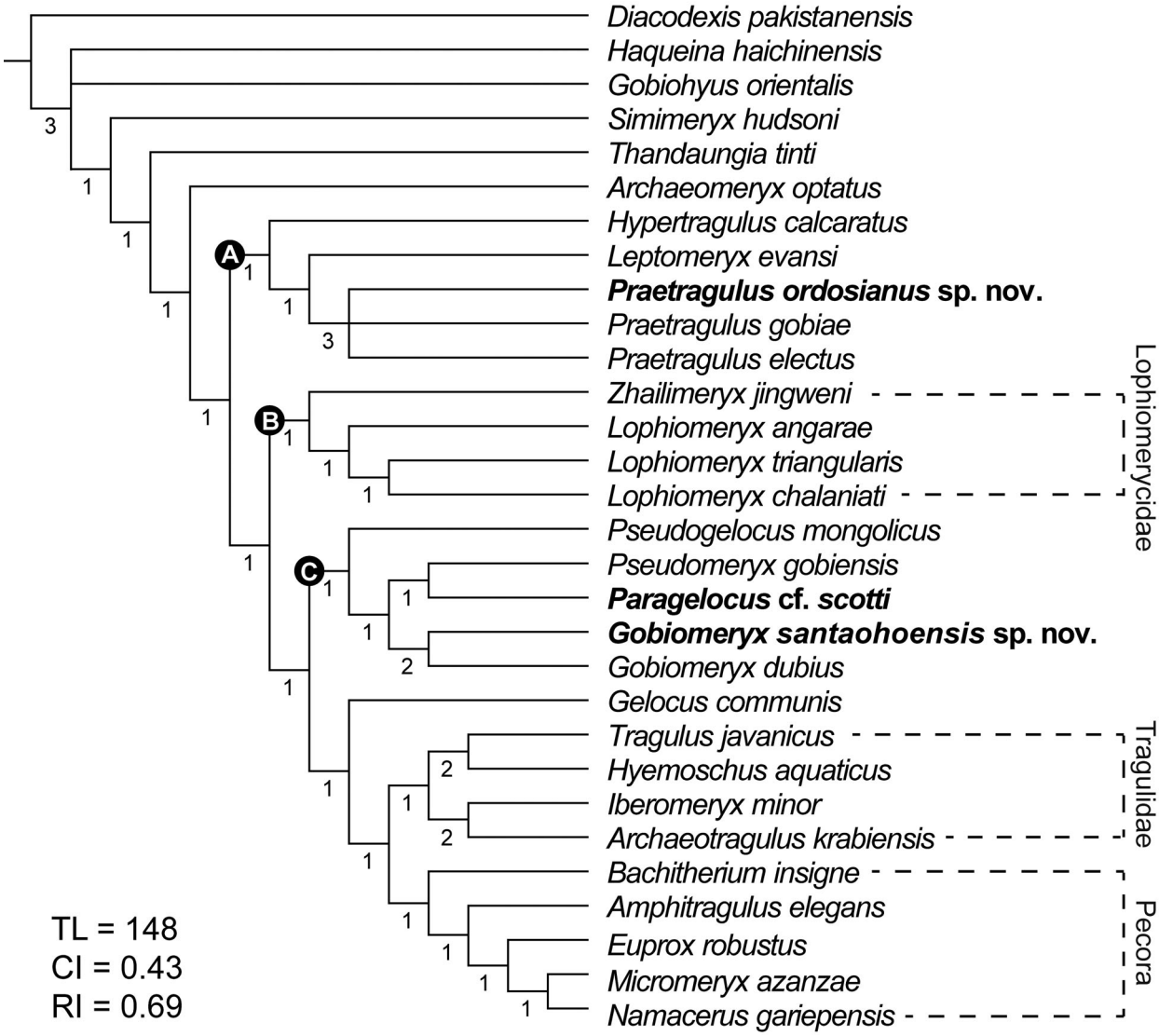

Figure 7. Strict consensus tree of three most parsimonious trees obtained from heuristic analysis in TNT v.1.6 (Goloboff & Morales, 2023). Bremer support values are calculated. See Supplemental Appendix A for the 52 dental and postcranial characters used and Supplemental Appendix B for the character-taxon matrix. Stem ruminants identified from Early Oligocene deposits of Saint Jacques (*Praetragulus*, *Lophiomeryx*, *Paragelocus* and *Gobiomeryx*) represent three different lineages. See Table 1 and text for the synapomorphies of clades A–C. Note that *Simimeryx*, formerly attributed to Hypertragulidae and Praetragulidae, does not cluster with *Hypertragulus* or *Praetragulus*. **Abbreviations: TL,** tree length; **CI,** consistency index and **RI,** retention index.

Table 1. Non-ambiguous synapomorphies of major clades in which stem ruminants from Saint Jacques belong. Clades A, B and C are labelled in Figure 7. Derived character states are in parentheses. See full character list in Supplemental Appendix A.

Clade A	
8 (1)	Upper molar postprotocrista: short and posteriorly oriented (0); long and labially oriented (1)
24 (1)	p4 posterolingual cristid: absent (0); present (1)
32 (1)	Molars postentocristid: absent (0); present and connected to the posthypocristid, thus closing the talonid posteriorly (1); present, and not connected to the posthypocristid (2)
Clade B	
11 (2)	Mesostyle: absent (0); weak to moderately developed (1); strong with a "pinched" appearance (2)
29 (0)	Premetacristid: absent (0); present (1)
Clade C	
13 (2)	Premetaconulecrista shape: simple (0); bifurcated (incipient) (1); bifurcated (well defined) (2)
31 (1)	Molars metastylid: absent (0); present (1)
32 (1)	Molars postentocristid: absent (0); present and connected to the posthypocristid, thus closing the talonid posteriorly (1); present, and not connected to the posthypocristid (2)

Phylogenetic relationships

Phylogenetic analysis yielded three most parsimonious trees of 148 steps (consistency index = 0.43, retention index = 0.69), from which a strict consensus tree was computed (Fig. 7). Aside from the non-ruminant artiodactyls from the Eocene of Asia (*Diacodexis pakistanensis*, *Gobiohyus orientalis* and *Haqueina haichinensis*), the assumed ruminants *Simimeryx hudsoni* and *Thandaungia tinti* are placed at the most basal part of the strict consensus tree. *Archaeomeryx optatus*, the earliest undisputed ruminant artiodactyl in Asia (Vislobokova & Trofimov, 2002), is differentiated from the basal taxa by the absence of paraconule (9^1) and by weakened posterior rib on upper molars (16^1). *Praetragulus* species are placed in a clade that also includes the North American taxa *Leptomeryx evansi* and *Hypertragulus calcaratus* (clade A; Fig. 7). Their synapomorphies include long and labially oriented postprotocrista (8^1), presence of p4 posterolingual cristid (24^1) and presence of postentocristid which connects with posthypocristid (32^1) (Table 1). *Zhailimeryx jingweni* forms a monophyletic group with *Lophiomeryx* species. Synapomorphies of this group (clade B) include well-developed mesostyle with a 'pinched' appearance (11^2) and absence of the premetacristid (29°).

The rest of the ruminant taxa included in the analysis are split into two lineages. The first lineage (clade C) includes *Pseudogelocus mongolicus*, *Pseudomeryx gobiensis*, *Paragelocus* cf. *scotti*, *Gobiomeryx dubius* and *Gobiomeryx santaohoensis* sp. nov. The monophyly of this clade is characterized by premetaconulecrista bifurcation on the upper molars (13^2) and the presence of a metastylid (31^1) and a postentocristid (32^1) on the lower molars (Table 1). *Paragelocus* cf. *scotti* is a sister taxon to *Pseudomeryx gobiensis*, united by the absence of posterolingual conid (23°) and the presence of a longitudinal cristid on p4 (28^1), with the latter being a derived character that is only present in these two taxa.

Gelocus communis was recovered as the basal offshoot of the other lineage, which also includes the sister clades of Tragulidae and Pecora. *Iberomeryx minor* and *Archaeotragulus krabiensis* are recovered as sister taxa, forming a monophyletic group with the extant tragulids *Tragulus javanicus* and *Hyemoschus aquaticus*. Pecoran taxa included in the analysis (*Bachitherium*, *Amphitragulus*, *Euprox*, *Micromeryx* and *Namacerus*) are recovered as a monophyletic group.

Discussion

Insights into the interrelationships of early ruminants

Resolving the phylogeny of early ruminants has been a challenging task given the limitation of the fossil record and the documented mosaic evolutionary pattern of this group, and the interrelationships of certain genera and families remain obscure through comparative morphology and phylogenetic analysis (Janis, 1987; Janis & Theodor, 2014). With regard to the ruminants described from the Saint Jacques-Qianlishan area in our recent study (Wang, B., Wang, et al., 2023) and the present study, we find that these taxa belong to three separate clades of non-pecoran ruminants. Specifically, *Praetragulus* clusters in a clade that also includes the North American genera *Leptomeryx* and *Hypertragulus*, *Lophiomeryx* is closely related to *Zhailimeryx*, while *Paragelocus* and *Gobiomeryx* cluster in a clade that also includes *Pseudomeryx* and *Pseudogelocus* (Fig. 7).

Praetragulus is notable for being considered by Vislobokova (1998, 2001) as the first indisputable member of the 'Hypertraguloidea' superfamily from Eurasia, based on its similarity with North American 'hypertraguloids'

(*Hypertragulus*, *Nanotragulus*, *Simimeryx*, *Parvitragulus* and *Hypisodus*) in cranial, dental and postcranial morphology (Métais & Vislobokova, 2007). The genus was originally included in Hypertragulidae (Vislobokova, 1998) but was later moved to a new family, Praetragulidae, along with the North American genera *Simimeryx* and *Parvitragulus* (Vislobokova, 2001). In our phylogenetic tree, *Praetragulus* is most closely related to *Leptomeryx*, which was regarded by Vislobokova (2001) and Métais and Vislobokova (2007) as a member of the superfamily 'Traguloidea'. This result renders the two superfamilies paraphyletic.

While Vislobokova (1998) considered *Simimeryx* among all 'hypertraguloids' to be most similar to *Praetragulus* in overall tooth morphology, she took note of the various osteological and dental differences between them and commented that "these genera do not appear to be closely related" (p. 16). In our phylogenetic result, *Simimeryx hudsoni* is more closely related to Eocene artiodactyls from Asia, namely *Thandaungia tinti* and *Archaeomeryx optatus*, lending support to the conclusion by Métais (2006) that an Asian origin of North American ruminants is rooted in late Eocene dispersal events. *Simimeryx* retains ancestral characteristics such as absence of mesostyle and very reduced M3 metaconule (Stock, 1934); its basal position in the strict consensus tree suggests that it may not be attributed to Praetragulidae or Hypertragulidae. Future phylogenetic analyses should involve more North American taxa as well as cranial morphology, to fully resolve their interrelationship as well as their relationships to Asian taxa.

Zhailimeryx jingweni, known from the late middle Eocene of central China, is widely considered the earliest and most primitive lophiomerycid ruminant (Guo et al., 2000; Métais & Vislobokova, 2007). In our strict consensus tree, the monophyly of *Zhailimeryx* and *Lophiomeryx* is supported (Fig. 7, Table 1). *Pseudomeryx*, *Pseudogelocus*, *Gobiomeryx* and *Paragelocus* have all been considered as members of the family 'Gelocidae', with *Gelocus communis* being the type species (Métais & Vislobokova, 2007; Vislobokova, 2001; Vislobokova & Daxner-Höck; 2002). The result of our phylogenetic analysis shows that *Gelocus* forms a paraphyletic group with the Asian 'gelocids' mentioned above. This renders the 'Gelocidae' a problematic clade, and its definition and composition require reconsideration.

The derived p4 morphology of *Paragelocus* cf. *scotti* in this study is highly similar to the p4 of *Pseudomeryx gobiensis* from the Valley of Lakes (NHMW 2001z0112/0001) (Vislobokova & Daxner-Höck; 2002). However, the p4 of *Pseudomeryx gobiensis* has more pronounced anterior bifurcation and a longer longitudinal cristid which ends at the posterolingual corner of the tooth. *Pseudomerys gobiensis* is closer in size to the smaller, more primitive p4 condition of *Paragelocus* cf. *scotti*, and *Pseudomeryx* sp. is similar in size with the more derived p4 of *Paragelocus* cf. *scotti* (Supplemental Table S3). The morphological affinity and close relationship of *Pseudomeryx*, and *Paragelocus* in our phylogenetic analysis may imply their congeneric status. Future attempts to resolve the relationship between these relatively poorly documented taxa should involve a detailed comparison of specimens from France, Mongolia and China.

Biochronology of *Praetragulus*, *Gobiomeryx* and *Paragelocus*

The type species of *Praetragulus*, *Praetragulus electus* Vislobokova, 1998, was discovered in the upper part of the Ergilin-Dzo Formation at Khoer-Dzan, eastern Mongolia, considered late Eocene in age based on mammalian fossil assemblage (Tsubamoto et al., 2022). The more primitive *P. gobiae* comes from the lower horizon of the Ergilin-Dzo Formation at the Ardyn Obo locality as well as from the early Oligocene Tatal-Gol locality, Mongolia (Matthew & Granger, 1925b; Métais & Vislobokova, 2007; Vislobokova, 1998). Additionally, Wang, B.-Y. et al. (1981) reported presence of *P. gobiae* (*Lophiomeryx gobiae*) from horizon no. 11 in Qianlishan, Nei Mongol, likely of late Eocene age, but no further information was given. *Praetragulus ordosianus* sp. nov. spans litho-units 5 through the lower part of litho-unit 8 at Saint Jacques (Fig. 1C). Small-mammal biostratigraphy suggests a late Early Oligocene age of these units (Wang, B., Zhang, et al. 2023; Wasiljeff & Zhang, 2022). This renders *Praetragulus ordosianus* sp. nov. the last species of the genus to appear and possibly also the last to survive.

Gobiomeryx is known from the late Eocene to early Oligocene of Central Asia (Métais & Vislobokova, 2007; Trofimov, 1957). The type species, *G. dubius*, is known from the early Oligocene of Mongolia and Kazakshstan (Musakulova, 1963; Vislobokova, 2001; Vislobokova & Daxner-Höck; 2002). Additionally, Vislobokova and Daxner-Höck (2002) reported upper and lower teeth of *Gobiomeryx* sp. from the early Oligocene of the Valley of Lakes, Mongolia. The only *Gobiomeryx* specimen previously reported from China is an m3 (IVPP V11481) from the late Middle Eocene Nadu Formation in Guangxi Province, assigned to *Gobiomeryx* sp. (Guo et al., 1999). *Gobiomeryx santaohoensis* sp. nov. only occurs in litho-unit 7 of Saint Jacques (Fig. 1C). It is younger than the occurrence of *G. dubius* in Mongolia (but partly overlaps with *G.* sp. from Mongolia) and the dental morphology is more derived than the latter by its increased size and crown height as well as better-developed entoconulid.

All materials referred to *Paragelocus* reported so far, including those from the present study, are from the early Oligocene of Eurasia (Métais & Vislobokova, 2007; Schlosser, 1902; Vislobokova & Daxner-Höck, 2002). In the Saint Jacques sequence, *Paragelocus* cf. *scotti* occurs in litho-unit 5 to 7, largely overlapping with *Praetragulus ordosianus* sp. nov. stratigraphically.

Diversity of stem ruminants in the Oligocene of Asia

One of the richest records of Oligocene ruminants known in Asia comes from the Valley of Lakes, central Mongolia. Stem ruminant fossils identified from fragmentary dental materials there include seven genera (*Praetragulus*, *Miomeryx*, *Gobiomeryx*, *Pseudomeryx*, *Pseudogelocus*, *Paragelocus* and *Lophiomeryx*) belonging in four lineages (Praetragulidae, Archaeomerycidae, 'Gelocidae' and Lophiomerycidae) (Vislobokova & Daxner-Höck, 2002), dominating the early Oligocene (biozones A–B) ruminant fauna in the Valley of Lakes. By the late Oligocene (biozone C), *Paragelocus* aff. *scotti* is the only stem ruminant remaining, and the ruminant fauna is largely replaced by stem Pecora (*Prodremotherium*, *Amphitragulus*, *Dremotherium*, *Palaeohypsodontus*) (Vislobokova & Daxner-Höck, 2002).

Previously, Oligocene ruminant fossils from China have been scarce (Métais & Vislobokova, 2007). However, extensive fieldwork conducted in the Saint Jacques-Qianlishan area over the past decade has revealed that Oligocene large-mammal fauna was more diverse than previously recognized. The total richness of stem ruminants at Saint Jacques now adds up to seven species belonging in four genera. Among these seven species, only *Lophiomeryx triangularis* is found in the late Oligocene, represented by an isolated molar from north-western China (Qiu, 1965; Wang, B., Wang, et al., 2023). At Saint Jacques, all stem ruminant fossils excavated so far are restricted to early Oligocene strata, while the late Oligocene strata have yielded fossil Pecora (unpublished data).

On the Mongolian Plateau and elsewhere in Asia, the late Oligocene fossil record of stem ruminants is highly limited, with sporadic occurrences of *Lophiomeryx* and early tragulids (Flerov, 1938; Métais & Vislobokova, 2007; Nanda & Sahni, 1990; Qiu, 1965; Wang, B., Wang, et al., 2023). Despite the climatic and environmental changes (Song et al., 2023; Sun et al., 2014; Wang, Y.-C., et al., 2023) and terrestrial mammalian faunal transition across the Eocene–Oligocene boundary known as the Mongolian Remodelling (Meng & McKenna,1998), new fossil evidence from the Mongolian Plateau implies that the main faunal turnover of early ruminants in this region occurred across the boundary between Early Oligocene and Late Oligocene (~28 Ma), long after the E/O transition. The emergence of several pecoran clades in the Late Oligocene possibly marks an important change in the ruminant faunal composition.

Conclusions

We identified three species of stem ruminants based on abundant fossil jaws and teeth collected from the Saint Jacques-Qianlishan area, Nei Mongol: *Praetragulus ordosianus* sp. nov., *Gobiomeryx santaohoensis* sp. nov. and *Paragelocus* cf. *scotti*. Both new species represent the last members of their respective genera. With this new collection and the previously reported *Lophiomeryx* fossils from the same strata, the study area has yielded seven species of Oligocene stem ruminants belonging to four genera and three different lineages. This marks one of the richest stem Ruminantia fossil records in Asia and provides important information about the early evolution of ruminants.

Our phylogenetic analysis based on 52 dental and postcranial characters supports the placements of *Praetragulus ordosianus* sp. nov. and *Gobiomeryx santaohoensis* sp. nov. at the genus level, and it suggests a close relationship between *Paragelocus* cf. *scotti* and several other 'gelocids', especially *Pseudomeryx*, despite the probable polyphyly of this poorly defined group.

Fossil evidence from China and Mongolia shows that early ruminants, since their emergence and diversification in the Eocene of Asia, continued to flourish on the Mongolian Plateau in the early Oligocene. With the exception of *Lophiomeryx* (which survived into the late Oligocene) and the Tragulidae (which is the only non-pecoran lineage remaining today), most of these early lineages last occurred in Asia in the late early Oligocene. The diversity of stem ruminants rapidly declined in the late Oligocene.

Acknowledgements

We thank Yuan-Qing Wang, Bin Bai and Qian Li for their helpful discussions on this work; the many individuals who participated in field work and fossil collection over the years (Wei Zhou, Yong-Xing Wang, Yong-Fu Wang, Shi-Jie Li, Yuan-Qing Wang, Bin Bai, Hai-Bing Wang, Yan Liu, Li-Qun Shi, Fang-Yuan Mao, Li-Ping Dong, Hai-Dan Ma, Jian Wang, Li-Hua Wang, Wei Gao and Ping Wang); Wei Zhou for fossil preparation; and Wei Gao for photography. We also thank Israel M. Sánchez, Bastien Mennecart and Romain Weppe for their constructive feedback and

expertise, which helped improve the quality of the manuscript. This study was funded by the National Natural Science Foundation of China (42402010, 42472015 and 41472003), the State Key Laboratory of Palaeobiology and Stratigraphy (Nanjing Institute of Geology and Palaeontology, Chinese Academy of Sciences) (223128), the Strategic Priority Research Program of Chinese Academy of Sciences (XDB26000000) and the Special Fund for Fossil Excavation and Preparation of the Chinese Academy of Sciences.

Declaration of interest statement

The authors report there are no competing interests to declare.

Supplemental material

Supplemental material for this article can be accessed here: https://doi.org/10.1080/14772019.2025.2552230.

Data availability statement

The data that support the findings of this study are openly available in MorphoBank at https://doi.org/10.7934/P5990 (Wang, B. et al., 2025).

References

Bärmann, E. V., & **Rössner, G. E.** (2011). Dental nomenclature in Ruminantia: towards a standard terminological framework. *Mammalian Biology*, *76*(6), 762–768. https://doi.org/10.1016/j.mambio.2011.07.002

Becker, D., **Lapaire, F.**, **Picot, L.**, **Engesser, B.**, & **Berger J.-P.** (2004). Biostratigraphie et paléoécologie du gisement à vertébrés de La Beuchille (Oligocène, Jura, Suisse). *Revue de Paléobiologie, Genève*, *9*, 179–191.

Bouvrain. G., **Geraads, D.**, & **Sudre J.** (1986). Révision taxonomique de quelques ruminants oligocènes des phosphorites du Quercy. *Comptes Rendus de l'Académie des Sciences, Paris, Series* II, *302*, 101–104.

Boyd, C. A., & **Welsh, E.** (2014). Description of an earliest Orellan fauna from Badlands National Park, Interior, South Dakota and implications for the stratigraphic position of the Bloom Basin limestone bed. *Dakoterra*, *6*, 124–147.

Brunet, M., & **Sudre, J.** (1987). Evolution et systematique du genre *Lophiomeryx* POMEL 1853 (Mammalia, Artiodactyla). *Münchner Geowissenschaftliche Abhandlungen*, *10*, 225–242.

Colbert, E. H. (1941). The osteology and relationships of *Archaeomeryx*, an ancestral ruminant. *American Museum Novitates*, *1135*, 1–24.

Coombs, M. C., & **Coombs, W. P.** (1977). Dentition of *Gobiohyus* and a reevaluation of the Helohyidae (Artiodactyla). *Journal of Mammalogy*, *58*(3), 291–308. https://doi.org/10.2307/1379328

Dong, W., **Liu, J.-H.**, & **Pan, Y.-R.** (2003). A new *Euprox* from the Late Miocene of Yuanmou, Yunnan Province, China, with interpretation of its paleoenvironment. *Chinese Science Bulletin*, *48*(5), 485–491. https://doi.org/10.1360/03tb9103

Ducrocq, S. (2019). *Pakkokuhyus* and *Progenitohyus* (Artiodactyla, Mammalia) from the Eocene of Southeast Asia are not Helohyidae: paleobiogeographical implications. *PalZ*, *93*, 105–113. https://doi.org/10.1007/s12542-018-0425-5

Ducrocq, S., **Chaimanee, Y.**, **Chavasseau, O.**, **Soe, A. N.**, **Sein, C.**, & **Jaeger J. J.** (2023). New material of *Paukkaungmeryx minutus* (Cetartiodactyla, Archaeomerycidae) from the late Middle Eocene Pondaung Formation, Myanmar. *Vertebrata PalAsiatica*, *61*(3), 182–197.

Ducrocq, S., **Chaimanee, Y.**, **Jaeger, J. J.**, **Yamee, C.**, **Rugbumrung, M.**, **Grohé, C.**, & **Chavasseau, O.** (2021). New fossil remains from Bang Mark locality, Krabi Basin, southern Thailand. *Journal of Vertebrate Paleontology*, *41*(4), e1988624. https://doi.org/10.1080/02724634.2021.1988624

Flerov, K. K. (1938). On the remains of Ungulata from the Betpakdala. *Doklady Akademii Nauk SSSR*, *21*, 95–96. [In Russian]

Geraads, D., **Bouvrain, G.**, & **Sudre, J.** (1987). Relations phyletiques de *Bachitherium* Filhol, ruminant de l'Oligocène d'Europe occidentale. *Palaeovertebrata*, *17*(2), 43–73.

Goloboff, P., & **Morales, M.** (2023). TNT version 1.6, with a graphical interface for MacOs and Linux, including new routines in parallel. *Cladistics*, *39*, 144–153. https://doi.org/10.1111/cla.12524

Guo, J.-W., **Dawson, M. R.**, & **Beard, K. C.** (2000). *Zhailimeryx*, a new lophiomerycid artiodactyl (Mammalia) from the late Middle Eocene of central China and the early evolution of ruminants. *Journal of Mammalian Evolution*, *7*(4), 239–258. https://doi.org/10.1023/A:1009433715125

Guo, J.-W., **Qi, T.**, & **Sheng, T.-J.** (1999). A restudy of the Eocene ruminants from Baise and Yongle basins, Guangxi, China, with a discussion of the systematic positions of *Indomeryx*, *Notomeryx*, *Gobiomeryx*, and *Prodremotherium*. *Vertebrata PalAsiatica*, *37*(1), 18–39.

Janis, C. M. (1987). Grades and clades in hornless ruminant evolution: the reality of the Gelocidae and the systematic position of *Lophiomeryx* and *Bachitherium*. *Journal of Vertebrate Paleontology*, *7*(2), 200–216. https://doi.org/10.1080/02724634.1987.10011653

Janis, C. M., & **Scott, K. M.** (1987). The interrelationships of higher ruminant families with special emphasis on the members of the Cervoidea. *American Museum Novitates*, *2893*, 1–85.

Janis, C. M., & **Theodor, J. M.** (2014). Cranial and postcranial morphological data in ruminant phylogenetics. *Zitteliana B*, *32*, 15–31.

Korth, W. W., & **Diamond, M. E.** (2002). Review of *Leptomeryx* (Artiodactyla, Leptomerycidae) from the Orellan (Oligocene) of Nebraska. *Annals of Carnegie Museum*, *71*(2), 107–129. https://doi.org/10.5962/p.215807

Kumar, K., **Rose, K. D.**, **Rana, R. S.**, **Singh, L.**, **Smith, T.**, & **Sahni, A.** (2010). Early Eocene artiodactyls (Mammalia) from western India. *Journal of Vertebrate Paleontology*, *30*(4), 1245–1274. https://doi.org/10.1080/02724634.2010.483605

Matthew, W. D., & **Granger, W.** (1925a). New mammals from the Irdin Manha Eocene of Mongolia. *American Museum Novitates*, *198*, 1–10.

Matthew, W. D., & **Granger, W.** (1925b). New ungulates from the Ardyn Obo Formation of Mongolia, with faunal list and remarks on correlation. *American Museum Novitates*, *195*, 1–12.

Meng, J., & **McKenna, M. C.** (1998). Faunal turnovers of Paleogene mammals from the Mongolian Plateau. *Nature*, *394*, 364–366. https://doi.org/10.1038/28603

Mennecart, B. (2012). The Ruminantia (Mammalia, Cetartiodactyla) from the Oligocene to the Early Miocene of Western Europe: systematics, palaeoecology and palaeobiogeography. *GeoFocus*, *32*, 1–263.

Mennecart, B. (2015). The European ruminants during the "*Microbunodon* Event" (MP28, latest Oligocene): impact of climate changes and faunal event on the ruminant evolution. *PLoS ONE*, *10*, e0116830. https://doi.org/10.1371/journal.pone.0116830

Mennecart, B., **Becker, D.**, & **Berger, J. P.** (2011). *Iberomeryx minor* (Mammalia, Artiodactyla) from the Early Oligocene of Soulce (Canton Jura, NW Switzerland): systematics and palaeodiet. *Swiss Journal of Geoscience*, *104*(1), 115–132. https://doi.org/10.1007/s00015-010-0034-0

Mennecart, B., & **Métais, G.** (2015). *Mosaicomeryx* gen. nov., a ruminant mammal from the Oligocene of Europe and the significance of 'gelocids.' *Journal of Systematic Palaeontology*, *13*(7), 581–600. https://doi.org/10.1080/14772019.2014.948505

Métais, G. (2006). New basal selenodont artiodactyls from the Pondaung Formation (late Middle Eocene, Myanmar) and the phylogenetic relationships of early ruminants. *Annals of Carnegie Museum*, *75*(1), 51–67. https://doi.org/10.2992/0097-4463(2006)75[51:NBSAFT]2.0.CO;2

Métais, G., **Chaimanee, Y.**, **Jaeger, J. J.**, & **Ducrocq, S.** (2001). New remains of primitive ruminants from Thailand: evidence of the early evolution of the Ruminantia in Asia. *Zoological Scripta*, *30*(4), 231–248. https://doi.org/10.1046/j.0300-3256.2001.00071.x

Métais, G., **Mennecart, B.**, & **Roohi, G.** (2017). A new assemblage of stem pecoran ruminants from the Oligocene Chitarwata Formation, Bugti Hills, Baluchistan, Pakistan: paleoenvironmental and paleobiogeographic implications. *Journal of Asian Earth Sciences*, *136*, 40–49. https://doi.org/10.1016/j.jseaes.2016.09.009

Métais, G., & Vislobokova I. A. (2007). Basal ruminants. In D. R. Prothero & S. E. Foss (Eds.), *The Evolution of artiodactyls* (pp. 189–212). Johns Hopkins University Press.

Métais, G., **Welcomme, J. L.**, & **Ducrocq S.** (2009). New lophiomerycid ruminants from the Oligocene of the Bugti Hills (Balochistan, Pakistan). *Journal of Vertebrate Paleontology*, *29*(1), 231–241. https://doi.org/10.1671/039.029.0115

Morales, J., **Soria, D.**, **Pickford, M.**, & **Nieto, M.** (2003). A new genus and species of Bovidae (Artiodactyla, Mammalia) from the early Middle Miocene of Arrisdrift, Namibia, and the origins of the family Bovidae. *Memoir of the Geological Survey of Namibia*, *19*, 371–384.

Musakulova, L. T. (1963). *Gobiomeryx* from the Paleogene of Kazakhstan. *Materialy po Istorii Fauny I Flory Kazakhstana*, *4*, 201–203.

Nanda, A. C., & **Sahni, A.** (1990). Oligocene vertebrates from the Ladakh Molasse Group, Ladakh Himalaya: paleobiogeographic implications. *Journal of Himalayan Geology*, *1*, 1–10.

Owen, R. (1848). Description of teeth and portions of jaws of two extinct anthracotherioid quadrupeds (Hyopotamus vectianus and Hyop. bovinus) discovered by the Marchioness of Hastings in the Eocene deposits on the NW coast of the Isle of Wight: with an attempt to develop Cuvier's idea of the classification of pachyderms by the number of their toes. *Quarterly Journal of the Geological Society*, *4*, 103–141.

Qiu, Z.-X. (1965). First discovery of *Lophiomeryx* in China. *Vertebrata PalAsiatica*, *9*(4), 395–398.

Sánchez, I. M., & **Morales, J.** (2008). *Micromeryx azanzae* sp. nov. (Ruminantia: Moschidae) from the middle-upper Miocene of Spain, and the first description of the cranium of *Micromeryx*. *Journal of Vertebrate Paleontology*, *28*(3), 873–885. https://doi.org/10.1671/0272-4634(2008)28[873:MASNRM]2.0.CO;2

Schlosser, M. (1902). Beiträge zur Kenntniss der Säugethierreste aus den süddeutschen Bohnerzen. *Geologische und palaeontologische Abhandlungen*, *5*(3), 1–144.

Scopoli, J. A. (1777). *Introdvctio ad historiam natvralem sistens genera lapidvm, plantarvm, et animalivm hactenvs detecta, caracteribvs essentialibvs donata, in tribvs divisa, svbinde ad leges natvrae*. Pragae.

Scott, K. M., & **Janis, C. M.** (1992). Relationships of the Ruminantia (Artiodactyla) and analysis of the characters used in ruminant taxonomy. In F. S. Szalay, M. J. Novacek, & M. C. McKenna (Eds.), *Mammal Phylogeny, Placentals* (pp. 282–302). Springer.

Song, S., **Tang, Z.**, **Xi, D.**, & **Yang, S.** (2023). Palynology-based reconstructions for climatic patterns in the Eocene–Oligocene of eastern Asia: Implications of the monsoonal circulation history. *Journal of Asian Earth Sciences*, *257*, 105836. https://doi.org/10.1016/j.jseaes.2023.105836

Stock, C. (1934). A hypertragulid from the Sespe Uppermost Eocene, California. *Proceedings of the National Academy of Sciences*, *20*(12), 625–629. https://doi.org/10.1073/pnas.20.12.625

Sudre, J. (1984). *Cryptomeryx* Schlosser, 1886, tragulidé de l'Oligocène d'Europe; relations du genre et considérations sur l'origine de ruminants. *Palaeovertebrata*, *14*(1), 1–31.

Sun, J., **Ni, X.**, **Bi, S.**, **Wu, W.**, **Ye, J.**, **Meng, J.**, & **Windley, B. F.** (2014). Synchronous turnover of flora, fauna and climate at the Eocene–Oligocene Boundary in Asia. *Scientific Reports*, *4*, 7463. https://doi.org/10.1038/srep07463

The Mesquite Project Team. (2023). *Documentation for Mesquite: a modular system for evolutionary analysis*. http://www.mesquiteproject.org

Thewissen, J. G. M., & **Hussain, S. T.** (1990). Postcranial osteology of the most primitive artiodactyls *Diacodexis pakistanensis* (Dichobunidae). *Anatomia, Histologia, Embryologia*, *19*(1), 37–48. https://doi.org/10.1111/j.1439-0264.1990.tb00876.x

Thewissen, J. G. M., **Russell, D. E.**, **Gingerich, P. D.**, & **Hussain, S. T.** (1983). A new dichobunid artiodactyl (Mammalia) from the Eoceneof north-west Pakistan. *Proceedings of the Koninklijke Nederlandse Akademie van Wetenschappen B*, *86*(2), 153–180.

Trofimov, B. A. (1957). Nouvelles données sur les Ruminantia les plus anciens d'Asie. *Cursillos y Conferiencias del Instituto "Lucas Mallada"*, *4*, 137–141.

Tsubamoto, T., **Tsogtbaatar, K.**, **Chinzorig, T.**, & **Egi, N.** (2022). A brief review of the updated fossil vertebrate fauna of the upper Eocene Ergilin Dzo Formation, southeastern Mongolia. *Memoirs of the Faculty of Science, Ehime University*, *24*, 64–83.

Vislobokova, I. A. (1998). A new representative of the Hypertraguloidea (Tragulina, Ruminantia) from the Khoer-Dzan locality in Mongolia, with remarks on the relationships of the Hypertragulidae. *American Museum Novitates*, *3225*, 1–24.

Vislobokova, I. A. (2001). Evolution and classification of Tragulina (Ruminantia, Artiodactyla). *Paleontological Journal*, *35*(Supp 2), S69–S145.

Vislobokova, I. A. (2004). A new representative of the family Raoellidae (Suiformes) from the Middle Eocene of Khaichin-Ula 2, Mongolia. *Paleontological Journal*, *38*(2), 220–226.

Vislobokova, I. A., & **Daxner-Höck, G.** (2002). Oligocene-early Miocene ruminants from the Valley of Lakes (Central Mongolia). *Annalen des Naturhistorischen Museums in Wien*, *103A*, 213–235.

Vislobokova, I. A., & **Trofimov, B. A.** (2002). *Archaeomeryx* (Archaeomerycidae, Ruminantia): morphology, ecology, and role in the evolution of the Artiodactyla. *Paleontological Journal*, *36*(Supp 5), S428–S523.

Wang, B., **Wang, Q.**, & **Zhang, Z.-Q.** (2023). New materials of *Lophiomeryx* (Artiodactyla: Lophiomerycidae) from the Oligocene of Nei Mongol, China. *Journal of Mammalian Evolution*, *30*, 1047–1066. https://doi.org/10.1007/s10914-023-09691-3

Wang, B., **Wang, Q.**, **Zhang, Z.** (2025). Project 5990: New early ruminants (Mammalia: Artiodactyla) from the Oligocene of Nei Mongol (China), with remarks on their phylogenetic relationship [Dataset]. *Morphobank*. https://doi.org/10.7934/P5990

Wang, B., **Zhang, Z.-Q.**, **Wang, Y.-Q.**, **Li, Q.**, **Bai, B.**, **Liu, Y.**, **Mao, F.-Y.**, **Wang, H.-B.**, **Wang, J.**, **Gong, Y.-X.**, **Dong, L.-P.**, **Wang, L.-H.**, **Ma, H.-D.**, **Xu, R.-C.**, & **Wang, X.-Y.** (2023). Lithostratigraphy of a long, fossiliferous Oligocene sequence: Revisiting Saint Jacques, Nei Mongol, China. *Frontiers in Earth Science*, *11*, 1127964. https://doi.org/10.3389/feart.2023.1127964

Wang, B.-Y., **Chang, J.**, **Meng, X.-J.**, & **Chen, J.-R.** (1981). Stratigraphy of the upper and middle Oligocene of Qianlishan district, Nei Mongol (Inner Mongolia). *Vertebrata PalAsiatica*, *19*(1), 26–34.

Wang, S.-Q., **Ji X.-P.**, **Zhang, C.-X.**, **Wang, Y.**, **Chen, G.-Y.**, **Hu, Z.-G.**, & **Yang H.-F.** (2025). A new dichobunoid artiodactyl from the middle Eocene of Yunnan, China. *Palaeoworld*, *34*(2). https://doi.org/10.1016/j.palwor.2024.100874

Wang, Y.-C., **Lu, H.-Y.**, **Lyu, H.-Z.**, **Cai, D.-X.**, **Qiang, X.-K.**, **Li, Y.-X.**, **Wang, X.-Y.**, **Lai, W.**, **Wang, Y.**, **Zhang, H.-Z.**, **Wang, K.-X.**, **Huang, Z.-H.**, **Yu, X.-C.**, & **Hu, S.-L.** (2023). East Asian hydroclimate responses to the Eocene–Oligocene transition in the Weihe Basin, central China. *Palaeogeography, Palaeoclimatology, Palaeoecology*, *615*, 111436. https://doi.org/10.1016/j.palaeo.2023.111436

Wasiljeff, J., & **Zhang, Z.-Q.** (2022). Stratigraphical significance of Ulantatal sequence (Nei Mongol, China) in refining the latest Eocene and Oligocene terrestrial regional stages. *Vertebrata PalAsiatica*, *60*(1), 42–53.

Webb, S. D., & **Taylor, B. E.** (1980). The phylogeny of hornless ruminants and a description of the cranium of *Archaeomeryx*. *Bulletin of the American Museum of Natural History*, *167*, 117–158.

Associate Editor: Dr Jérémy Tissier